

# THz and FIR Spectroscopy

R. Bratschitsch, W. Fischler, R.A. Höpfel, R. Kersting, T. Müller,  
G. Strasser, J. Ulrich, K. Unterrainer, R. Zobl

Institut für Festkörperelektronik, Technische Universität Wien,  
Floragasse 7, A-1040 Vienna, Austria

## 1. Coherent THz emission from optically pumped parabolic quantum wells

(R. Bratschitsch, T. Müller, R. Kersting, G. Strasser, K. Unterrainer)

We present experiments which show that modulation doped parabolic quantum wells (PQWs) emit coherent THz radiation corresponding to the intersubband plasmon when excited by near infrared femtosecond laser pulses. The samples used in the experiments are modulation doped GaAs/AlGaAs PQWs, with widths in the range of 1200 - 2000 Å and carrier sheet densities of  $1.7 \times 10^{11} - 5 \times 10^{11} \text{ cm}^{-2}$ . We perform THz autocorrelation (AC) measurements using near infrared laser pulses. The Fourier transform of the recorded AC signal gives the spectrum of the coherent THz radiation emitted by the PQW.

Figure 1 shows the spectrum of a modulation doped PQW ( $W = 1400 \text{ Å}$ ,  $n_{2D} = 5 \times 10^{11} \text{ cm}^{-2}$ ) excited by 780 nm ( $\tau = 80 \text{ fs}$ ) laser pulses. The density of the optically generated carriers is kept well below the carrier density due to the modulation doping inside the PQW.

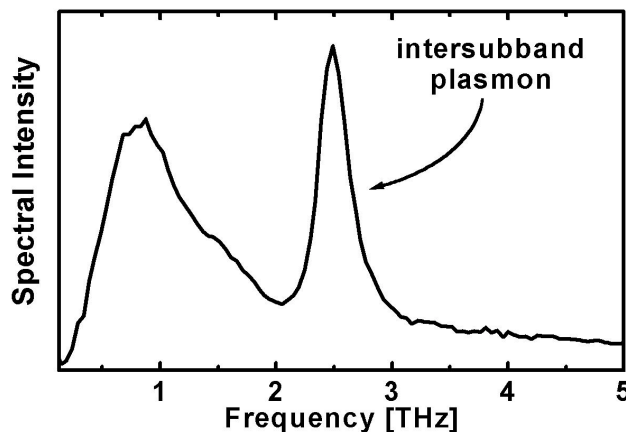


Fig. 1: THz emission of the 1400 Å PQW excited by 780 nm laser pulses ( $T = 5 \text{ K}$ ).

The spectrum of the emitted THz radiation consists of two components, a broad one around 0.8 THz due to THz generation at the surface of the sample and a narrow one (FWHM: 0.3 THz) with a center frequency of 2.55 THz. The narrowband emission results from the oscillation of the carriers inside the PQW at the intersubband plasmon

frequency. The narrowband PQW emission can be excited within a wide range of excitation wavelengths (815 – 760 nm). The combination of the designability of the transition frequency, the narrowband emission, and the absence of any processing of the sample make modulation doped PQWs attractive and easy-to-use THz emitters.

## 2. Few-cycle MIR emission from quantum beats

(T. Müller, R. Bratschitsch, G. Strasser, K. Unterrainer)

We report on the emission of few-cycle mid-infrared radiation from coherent charge oscillations in a semiconductor quantum well. We use 10 fs optical pulses to excite two quantized states in an asymmetric step quantum well, which was designed to maximize the optical interband and intersubband matrix elements. The coherent excitation of these states creates a coherent superposition of eigenstates. The polarization associated with the transitions then shows quantum beats due to the different energies of the transitions involved. The spacing of the two quantum states is 140 meV which corresponds to a beat frequency of about 33 THz. Even at room temperature more than 15 cycles of the oscillation can be observed before dephasing. The spectrum of the emitted radiation is obtained by an autocorrelation measurement. Fourier transform of the autocorrelation trace then gives the spectrum, which agrees very well with the results obtained from the numerical solution of the Liouville equation.

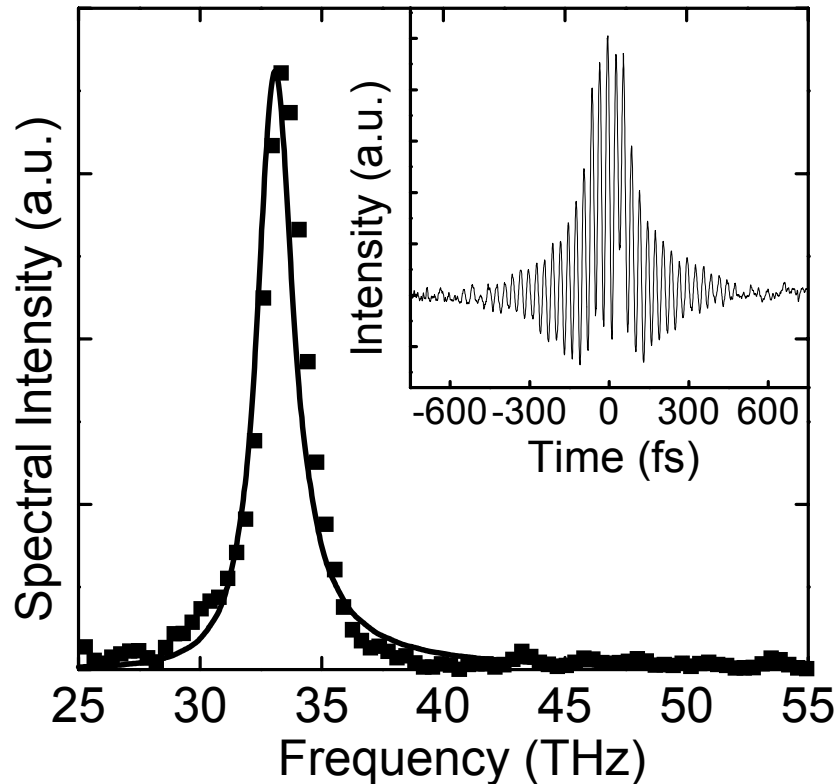


Fig. 2: The figure shows the measured (squares) and the calculated (line) spectrum of the emitted MIR radiation at room temperature. The autocorrelation signal is shown in the inset.

### 3. THz modulators and varactors

(R. Kersting, R. Bratschitsch, G. Strasser, K. Unterrainer (INTERACT collaboration))

We have shown in previous works that intersubband transitions in semiconductor heterostructures can be used to modulate free propagating THz pulses. However, modulation amplitudes have been low (1 – 5%). The purpose of the work was to design semiconductor heterostructures with increased modulation properties. The new structures have been grown by molecular beam epitaxy. Modulator devices have been fabricated and tested in terms of modulation amplitude and cut-off frequency. In addition, we performed time-resolved THz emission experiments on a varactor similar to that used by the RAL and Lille groups in their mixing experiments. We achieved the time-resolved data by photoexcitation of the varactor with 65 fs laser pulses at a wavelength of 800 nm. The excitation density is about  $5 \times 10^{16} \text{ cm}^{-3}$ . The THz pulse coming from the varactor was time-resolved by mixing the emission with a broadband THz pulse having a bandwidth of about 5 THz. The center frequency of the THz emission from the varactor was about 2.2 THz showing that the upper limit for the mixing technique could be around 2 THz.

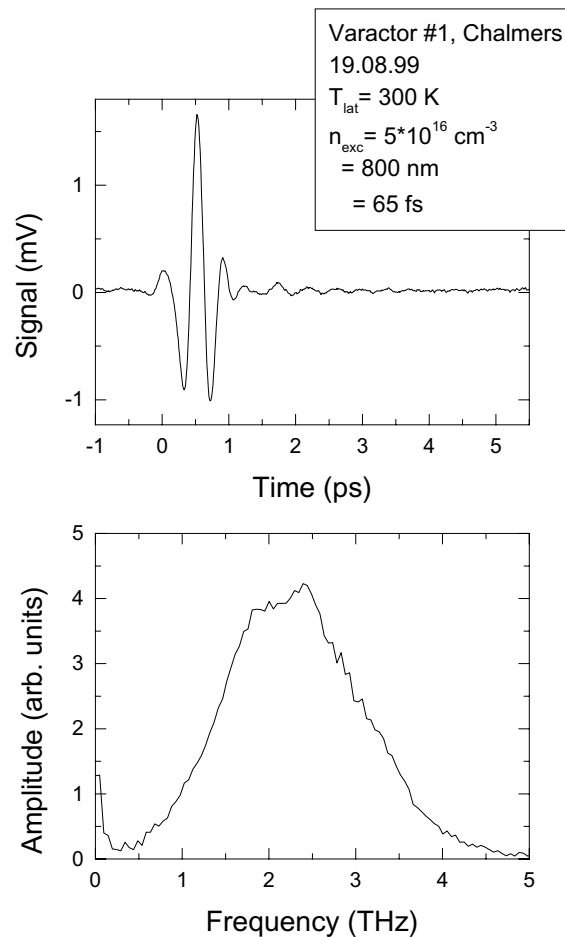
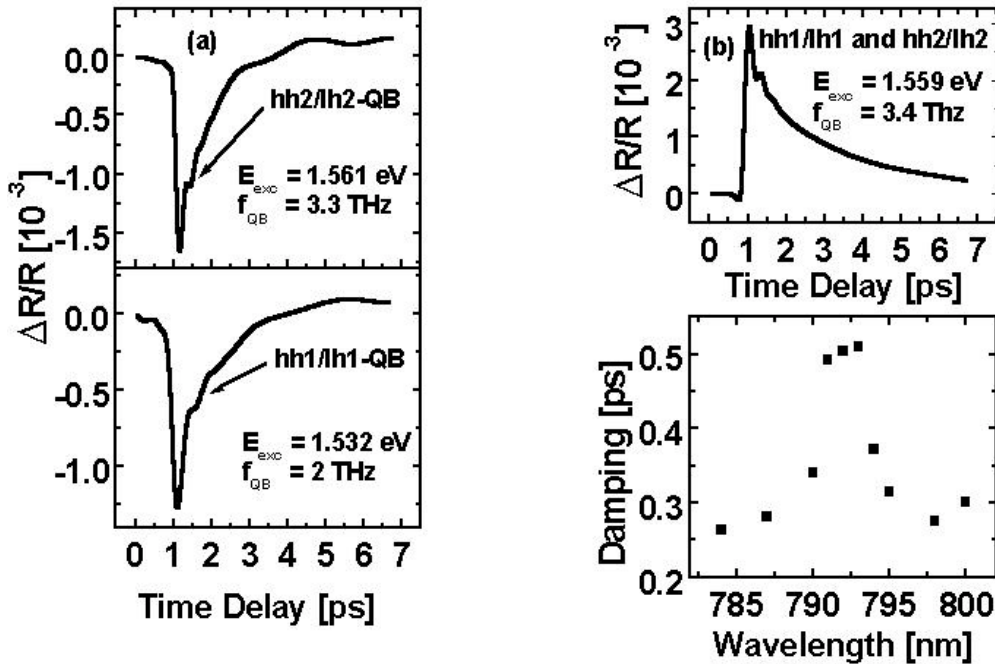


Fig. 3: The figure shows auto correlation and spectrum of the THz emission from a varactor similar to that used by the RAL and Lille groups in their mixing experiments. The varactor is excited with 65 fs laser pulses at a wavelength of 800 nm. The excitation density is about  $5 \times 10^{16} \text{ cm}^{-3}$ .

#### 4. Heavy hole/light hole quantum beats in symmetric and asymmetric double quantum wells

(W. Fischler, R.A. Höpfel, R. Bratschitsch, G. Strasser, K. Unterrainer)

We investigate optically excited quantum beats (QBs) in different GaAs/AlGaAs quantum well structures. The set of samples consists of symmetric double quantum wells (sDQW) and asymmetric double quantum wells (aDQW). Using a conventional pump-probe configuration (femtosecond near infrared pulses) we measure the time evolution of the change in sample reflectivity. Depending on the excitation energy we excite not only the well known QB between the first heavy hole and the first light hole electronic states (hh1/lh1-QB) but also a second one between the second heavy hole and light hole states (hh2/lh2-QB). In the case of an aDQW (Fig. 4(a)), both QBs are energetically separated and have different beat frequencies because of different hh-lh splittings in the wide and the narrow well. The damping times are constant over the energetic window where the QBs can be observed. In contrast, in the case of a sDQW the beat frequencies are nearly the same and the QBs are energetically not separated any more. But surprisingly, the signature of both QBs is revealed in a clear reduction of the measured damping when both oscillations are excited simultaneously. This behavior is interpreted as a consequence of the fact that the coherent polarizations of both QBs have the same sign and, therefore, interfere constructively.



(a)

(b)

Fig. 4: (a) aDQW: Reflectivity traces for two different excitation energies; (b) sDQW: Both QBs are simultaneously excited. Bottom: Reduction of damping.

## 5. Measurement of hot electron temperatures in parabolic quantum wells

(R. Zobl, J. Ulrich, G. Strasser, K. Unterrainer)

The validity of the Kohn theorem in PQWs was verified in a series of electroluminescence experiments (see Kohn). An additional magnetic field  $B$  whose axis was tilted at various angles with respect to the sample's growth axis was applied to produce the characteristic mode dispersion  $\omega_{\pm}(B)$  of two coupled harmonic oscillators (see Kohn, Fig. 5). In the measured FIR emission spectra the peak positions fully confirm the simple center of mass calculation (in the Heisenberg picture) for the dispersion. The FIR emission intensities  $I_d(\omega)$  therefore must follow the simple blackbody law  $I_{bb}(\omega, T_e)$  for an ensemble of pure harmonic oscillators radiating at the frequencies  $\omega_+$  and  $\omega_-$ , respectively. Since there are two easy to evaluate, background free emission lines, their absolute intensities together with their intensity ratio uniquely identify the electron temperatures  $T_e$  involved. The exact determination of  $T_e$  even by the use of an *uncalibrated* detector (i.e. with unknown responsivity V/W) therefore allows for a reasonable estimate about the actual terahertz radiation output of the wells (Fig. 5). At some 100 mW electrical input power electron temperatures exceed 70 K yielding an integral FIR emission in the  $10^{-7}$  W range per  $\text{cm}^2$  emissive area.

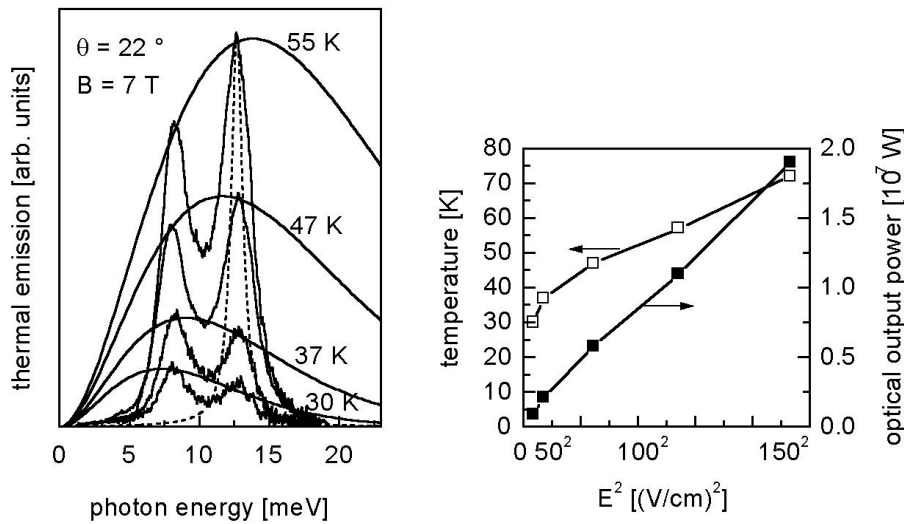


Fig. 5: Extraction of electron temperatures in a PQW: At  $\theta = 22^\circ$  magnetic field tilt angle and  $B = 7$  T the ‘oscillator strengths’  $f_{\pm}$  become equivalent with respect to the spatial orientation of the dipole oscillators corresponding to  $\omega_+$ ,  $\omega_-$ . The measured intensities, integrated over all contributing emission angles, then only differ by their blackbody weight  $I_{bb}(\omega_{\pm}, T_e)$ .

The left of Fig. 5 shows detected optical intensities  $I_d(\omega)$  for an electrical input power of 25 mW, 50 mW, 220 mW, and 510 mW. The dashed line represents a Lorentzian model of the emission lines with their actual FWHM linewidth of 1.1 meV. Planck’s radiation law  $I_{bb}(\omega, T_e)$  is plotted for the four electron temperatures  $T_e$  that satisfy  $I_d(\omega_{\pm}) = \alpha I_{bb}(\omega_{\pm}, T_e)$  using a common scaling factor  $\alpha$ . The right of Fig. 5 shows electron temperatures and optical output power vs  $E^2$  of electric driving field. No saturation in emission intensity is found.

## 6. Coherent THz plasmons in GaAs/AlGaAs superlattices

(R. Bratschitsch, R. Kersting, T. Müller, G. Strasser, and K. Unterrainer)

In contrast to the electrons in bulk material, the electrons in a superlattice reside inside a miniband. Depending on the miniband width (which can be designed by the well and barrier widths) the miniband can be filled with electrons to a certain level by doping the superlattice. In our experiments we use four different superlattices, 70 (50, 40, 40) periods of 50 Å (75, 100, 200) wells and 20 Å (20, 25, 25) barriers, with a width of the first electron miniband of 55 meV (26, 10, 2). The superlattices are all n-doped with  $n = 1 \times 10^{17} \text{ cm}^{-3}$ . This carrier concentration results in a filling percentage of the first electron miniband of 19% (39, 86, 100) (Fig. 6).

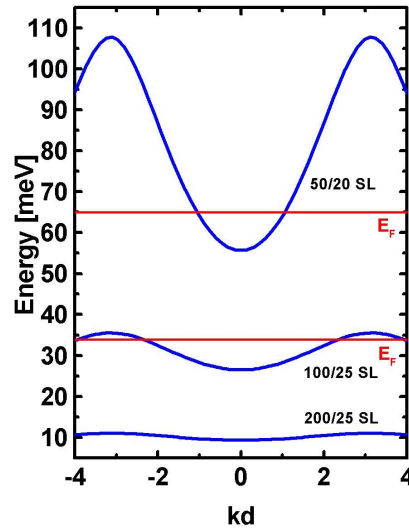


Fig. 6: First electron miniband for the 50/20, 100/25 and 200/25 superlattice. The Fermi energy is denoted by  $E_F$ .

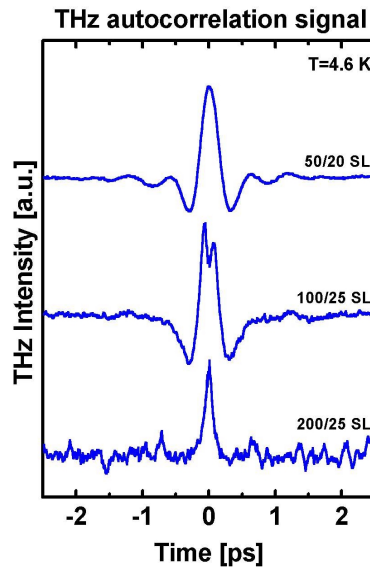


Fig. 7: THz autocorrelation signals of the 50/20, 100/25, and 200/25 superlattices, recorded at  $T = 4.6 \text{ K}$ .

Figure 7 shows the THz autocorrelation function for the three different superlattices recorded at  $T = 4.6$  K. While the autocorrelation signal for the superlattice with the full electron miniband (200/25) shows no oscillation the electrons in the 100/25 superlattice (86% miniband filling) begin to oscillate but this oscillation is strongly damped. For the 50/20 superlattice with a miniband filling of 19%, several oscillations can be seen. The frequency of the oscillations in the 50/20 superlattice is dependent on the optically generated carrier density ( $n_{\text{opt}} = 1 \times 10^{16} - 1 \times 10^{18} \text{ cm}^{-3}$ ). However, this dependence cannot be explained by a simple plasma frequency formula where the bulk effective mass of the electron is replaced by the effective mass of the electron inside the miniband.

In contrast to the THz emission experiments mentioned above, electrons that are optically generated by a femtosecond laser pulse can also perform plasma oscillations in a previously empty miniband. For this purpose we used the 200/25 superlattice which has a full first electron miniband but an empty second one. If the wavelength of the exciting laser pulses is tuned above the second miniband a strongly damped oscillation of the injected electrons appears.

Thermal saturation of a superlattice can be established if the thermal energy  $k_B T$  becomes larger than the miniband width. In this case the miniband becomes uniformly occupied although not full and the conductivity (mobility) decreases drastically. This decrease in mobility should also be seen in the THz oscillations. Two superlattices with a miniband width of 55.4 meV and 26.2 meV were grown and the THz autocorrelation functions were recorded for both samples at  $T = 4.6$  K and 300 K. At low temperature both samples show distinct oscillations because in both cases the thermal energy  $k_B T$  is much smaller than the miniband width. At room temperature the superlattice with the wide miniband ( $\Delta = 55.4$  meV) still shows the oscillations because  $k_B T = 26$  meV is smaller than the miniband width but the oscillations in the superlattice with the narrow miniband are strongly damped because  $k_B T$  is as large as the miniband width.

In summary, we have shown that dopant electrons or optically injected electrons in a superlattice begin to oscillate when excited by femtosecond laser pulses. These plasmons can not only be detected at low temperature but also at  $T = 300$  K. The oscillations can be prevented when the miniband is nearly full or full or when the miniband is thermally saturated.